

Simulating High-Intensity Proton Beams in Nonlinear Lattices with PyORBIT

S. Webb*, D. Bruhwiler, D. Abell, K. Danilov, J. R. Cary, Tech-X Corp., Boulder, CO 80303, USA
 S. Nagaitsev, A. Valishev, FNAL, Batavia, IL 60510, USA
 V. Danilov, A. Shishlo, ORNL, Oak Ridge, TN 73831, USA

Abstract

High-intensity proton linacs and storage rings are essential for a) state-of-the-art neutron source user facilities, b) extending the high-energy physics intensity frontier, c) as a driver to generate pions for a future neutrino factory or muon collider, and d) for transmutation of radioactive waste and associated energy production. For example, Project X at Fermilab will deliver MW proton beams at energies ranging from 3 to 120 GeV. Nonlinear magnetic lattices with large tune spreads and with integrable, nearly integrable and chaotic dynamics have been proposed to maximize dynamic aperture and minimize particle loss. We present PyORBIT simulations of proton dynamics in such lattices, including the effects of transverse space charge for the first time.

INTRODUCTION

High intensity storage rings such as the accumulator ring at the Spallation Neutron Source (SNS) are required to keep under 1 W/m of beam loss to avoid excessive radioactivation of the surrounding hardware. Due to intensity-driven effects, such as halo formation, this places a hard limit on the beam current and energies available at the intensity frontier. In order to achieve increasing intensity, new methods of mitigating the intensity driven instabilities must be developed and tested both experimentally and numerically. Here we present results studying the effects of *nonlinear decoherence* in highly nonlinear lattices on halo formation using the PyORBIT tracking code [1].

The fundamental idea behind the work presented in [2] and [3] is that strongly nonlinear oscillators have very amplitude-dependent tunes. This amplitude dependence leads to nonlinear decoherence, which causes any collective oscillations of the beam to “smear out”, and for any particles that may initially be in some dangerous resonance to be driven to a nearby amplitude where its new tune is out of resonance. The underlying difficulty of achieving such nonlinear decoherence generically is that the resulting trajectories are typically chaotic and poorly bounded, which can lead to an increase in the dynamic aperture which can limit beam current further. By using lattices that are nearly integrable, or which have a Hamiltonian with one or two invariant quantities, these novel lattice concepts can achieve strong nonlinear decoherence while maintaining a bounded, and in the case of the integrable elliptic lattice (IEL) in Sec. V A of [2], fully integrable motion.

We focus on the IEL, which has two transverse invariants in the absence of dispersion. This lattice has been studied extensively in the single particle limit, and we here present the first results using space charge. To study the effects the nonlinear decoherence can have on a space charge driven instability, we consider a result of the particle-core model of halo formation [4, 5, 6] that finds rapid halo formation in the presence of a mismatched core oscillating with a matched pre-halo [7]. Particles in the pre-halo are swept out into large radius orbits in a linear lattice. To simulate this in the IEL, we used the PyORBIT tracking code developed by Oak Ridge National Laboratory.

PYORBIT CODE

PyORBIT is a particle-in-cell accelerator simulation code developed off the original ORBIT code [8], which has been used for the SNS ring design and in simulations of collective effects for SNS and other projects [9]. The new code, like the original ORBIT, has a two-level structure. Time consuming calculations are performed on C++, and a high level simulation flow control is implemented in a scripting language. In PyORBIT the outdated and unsupported Super Code is replaced by Python, an interpreted, interactive, object-oriented, extensible programming language.

At the present moment, the core of the PyORBIT code includes a Bunch class as a container for macro-particles coordinates and parameters, the TEAPOT-like [10] elements library and lattice classes to simulate rings and beam transport lines, a set of space charge modules, nonlinear lattice elements for integrable optics, collimation and foil injection models, an MPI library Python shell, and a linear accelerator model. In PyORBIT the ring or transport line accelerator lattices can be constructed by using MAD 8 [11] or SAD[12] input files or directly in the Python script. The PyORBIT space charge modules have 2D, 2.5D (with possible perfect conducting wall boundary conditions), and 3D Poisson solvers based on the Fourier convolution theorem and discrete transformation (FFT) and the method of images space charge force calculation suggested by Jones [13]. The existing space charge modules have a low scalability for parallel calculations, and the development of new methods and relocation of the existing original ORBIT methods are underway.

To simulate the IEL, we added a new PyORBIT element to represent the magnetic fields in Sec. V.A. of [2], which we refer to as the *elliptic element*, because the fields are naturally written in elliptic coordinates. Benchmarking of the

* swebb@txcorp.com

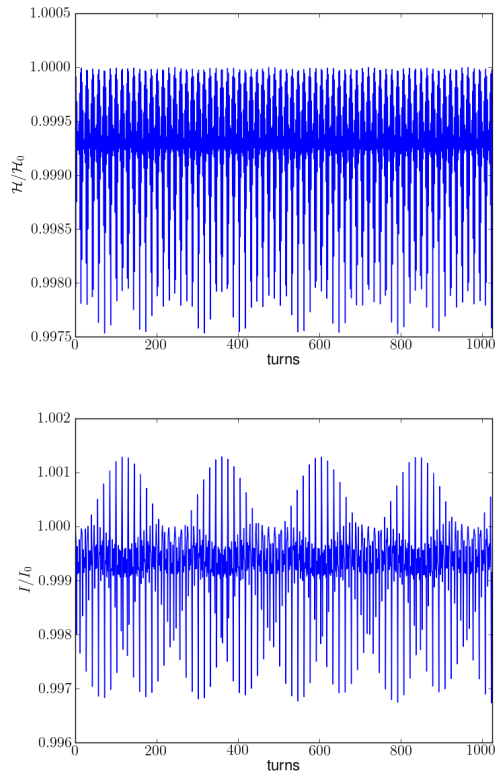


Figure 1: The Hamiltonian and second invariant are conserved to the order of 10^{-3} .

IEL lattice in an implementation with twenty discrete steps shows near conservation of both the Hamiltonian (eqn. 22 of [2]) and the second invariant (eqn. 20 of [2]) (see figure 1).

MATCHING & HALO FORMATION

The IEL lattice consists of a 2 meter elliptic element capped by a thin lens effective element that is focusing in both planes. It is necessary to have this to have equal beta functions in the horizontal and vertical plane to satisfy one of the conditions in [2].

Developing a scheme for matching a beam to the lattice proved crucial to studying the nonlinear elements. Matching with a Kapchinskij-Vladimirskij (KV) [14] distribution matched to the linear lattice leads to strong transient behavior in the IEL before arriving at a highly nonuniform distribution. To separate this dynamics from any halo formation, we developed a matching scheme for the IEL. In this sense, the matching is a fixed distribution of the single turn transfer map for the lattice.

Following in the spirit of the KV distribution, we considered a generalization that is a delta function of the elliptic Hamiltonian, and populated a phase space defined by

$$f(H(\vec{p}_N, \vec{q}_N)) = \delta(H(\vec{p}_N, \vec{q}_N) - \varepsilon_0) \quad (1)$$

where ε_0 reduces to the linear 4D emittance in the absence

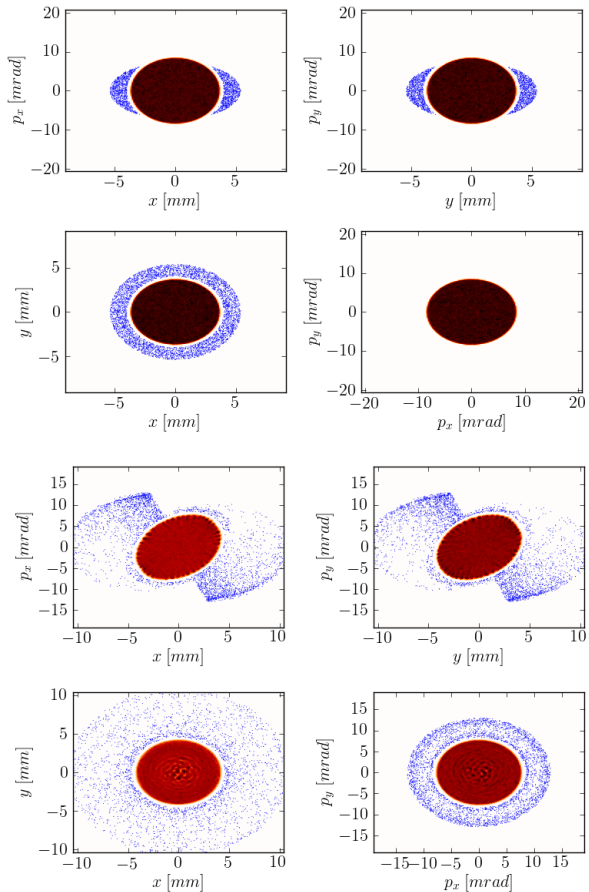


Figure 2: After 500 passes in the linear lattice, the initial pre-halo (top) has begun large radius oscillations (bottom).

of nonlinear elements, and \vec{p}_N and \vec{q}_N are the normalized accelerator coordinates described in, e.g., [15]. That any function of the invariants of motion is a fixed point of the Vlasov equation in the single-particle limit is well-known

Like the traditional KV distribution, this distribution uniformly fills a closed contour in every 2D projection. However, because of the nonlinear potential, the $x - y$ projection is no longer elliptical – it fills a contour defined by $V(x_N, y_N) = \varepsilon_0$ where V is the potential component of the Hamiltonian. For the IEL, this leads to an hourglass shape beam profile and, consequently, intrinsically nonlinear space charge forces.

To visualize the results of our tracking, we employed the matplotlib [16] Python plotting library. This library allows the use of \LaTeX , and generates publication-quality plots while interfacing conveniently with the SciPy/NumPy scientific Python libraries [17]. In the plots below, we overlay a histogram plot of the beam core (in red) with a scatter plot (blue dots) of particles outside 2 RMS momentum or position. The blue pre-halo dots are properly matched, and represent 1 % of the total beam current. In both cases, we considered a 100 A CW beam with approximately 2% linear tune depression. The lattice itself was a double-focusing

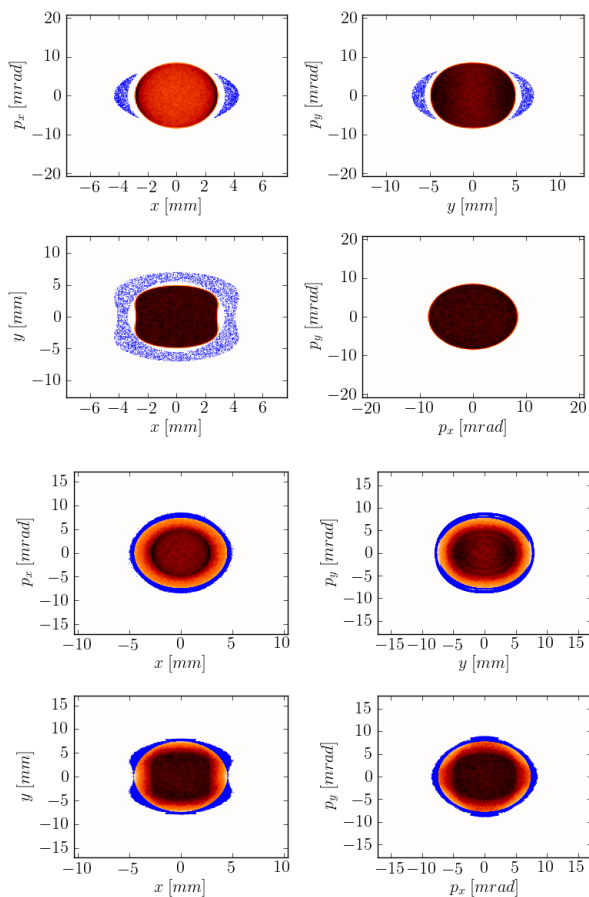


Figure 3: The initial (top) and equilibrium (bottom) beam with pre-halo in the IEL.

thin lens effective element, described in [2], with a two meter drift filled with the integrable elliptic element and a bare tune of 0.3

For the linear case (figure 2) we observe a rapid halo formation, where particles are swept out of the pre-halo and begin large radius oscillations out to twice the beam radius. This result keeps with the earlier result [7] regarding halo formation, and is a result of a parametric resonance caused by the breathing mode of the mismatched core.

By contrast (figure 3), the pre-halo in the IEL rapidly equilibrates with the core, reaching a new equilibrium in a very short time. This equilibrium is indistinguishable from the case where there was no pre-halo, just a mismatched core in the presence of space charge. We thus see that the strong nonlinearities present in the IEL suppress the formation of beam halo.

This result can be understood as coming from two mechanisms. First, because the individual particles in the core have different tunes, no coherent core breathing modes form. This contrasts with the linear case. Second, what coherent frequency content there is in the core oscillations can only drive a small fraction of the pre-halo particles resonantly for a short time before the nonlinear decoherence

takes those particles off resonance. Further details of this result have been submitted for publication [18, 19].

CONCLUSION

We have demonstrated, using the PyORBIT tracking code and Python-based visualization tools, that the nonlinear decoherence of the integrable elliptic lattice described in [2] prevents the formation of beam halo under circumstances well-known to generate beam halo in a linearly focusing lattice [7]. This intensity-dependent resonance is a major source of beam loss in intense beams, and its mitigation is crucial for the safe operation of high current beams. This is a promising first step towards the use of novel nonlinear lattice designs for the mitigation of beam current-driven instabilities, which will help develop next generation accelerator systems achieve increasing beam intensities.

ACKNOWLEDGEMENTS

This work was funded by the US DOE Office of Science, Office of High Energy Physics under grant No. DE-SC0006247.

REFERENCES

- [1] A. Shishlo, J. Holmes, and T. Gorlov, *Proc. of ICAP '09, THPSC052* (2009).
- [2] V. Danilov and S. Nagaitsev, *Phys. Rev. ST-AB* **13**, 84002 (2010).
- [3] K. Sonnad and J. Cary, *Phys. Rev. E* **69**, 056501 (2004).
- [4] J. O'Connell, T. Wangler, R. Mills, and K. Crandall, *Proc. of PAC '93*, pg. 3657-3659 (1993).
- [5] R. Gluckstern, *Phys. Rev. Lett.* **73**, 1247-1250 (1994).
- [6] R. Jameson, LANL Report LA-UR-94-3753 (1994).
- [7] D. Bruhwiler, AIP Conf. Proc. **377**, pg. 219-233 (1995).
- [8] J.A. Holmes *et al.*, ICFA Beam Dynamics Newsletter, **30** (2003), pp. 100-108.
- [9] A. Shishlo *et al.*, *Proc. of ICAP 2006*, pp. 53-58 (2006).
- [10] L. Schachinger and R. Talman, *Part. Accel.* **22** (1987), pp. 35-56.
- [11] <http://mad8.web.cern.ch/mad8>
- [12] <http://acc-physics.kek.jp/SAD>
- [13] F.W. Jones and H.O. Schönauer *Proc. of EPAC 2000*, pp. 1381-1383 (2000).
- [14] I. Kapchinskij and V. Vladimirskij, *Proc. of Int'l. Conf. on High Energy Acc.*, pg. 274-288 (1959).
- [15] S. Y. Lee, *Accelerator Physics*, 2nd ed., (2004).
- [16] J. Hunter in *Comp. in Sci. & Eng.*, **9**, 3 (2007).
- [17] E. Jones, T. Olipant, P. Peterson, *et al.*, <http://www.scipy.org>.
- [18] S. Webb, *et al.*, *Phys. Rev. Lett.*, submitted for publication.
- [19] S. Webb, *et al.*, *Phys. Rev. ST - Acc. Beams*, submitted for publication.